ACS APPLIED MATERIALS & INTERFACES

Research Article

www.acsami.org

Fabrication of a New Hydrous Zr(IV) Oxide-Based Nanocomposite for Enhanced Pb(II) and Cd(II) Removal from Waters

Ming Hua, Yingnan Jiang, Bian Wu, Bingcai Pan,* Xin Zhao, and Quanxing Zhang

State Key Laboratory of Pollution Control and Resource Reuse, School of the Environment, Nanjing University, Nanjing 210023, People's Republic of China

Supporting Information

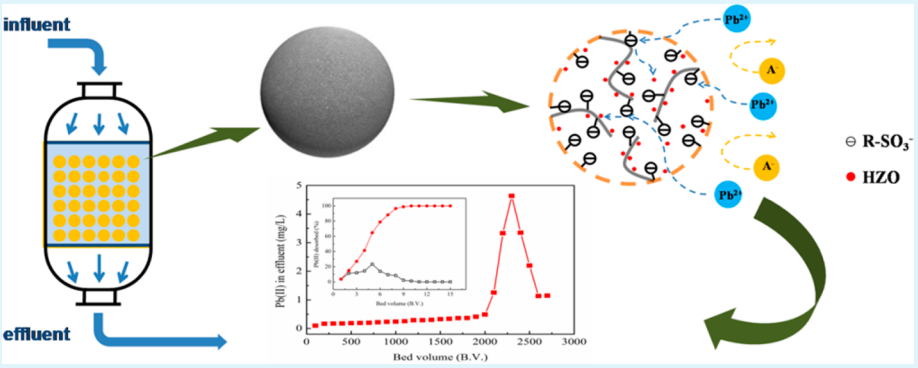

ABSTRACT: To overcome the technical bottleneck of fine hydrated Zr(IV) oxide particles in environmental remediation, we irreversibly impregnated nanosized hydrated Zr(IV) oxide inside a commercial cation exchange resin D-001 and obtained a new nanocomposite NZP. NZP exhibited efficient removal of lead and cadmium ions in a pH range of 2−6, where no Zr(IV) leaching was detected from NZP. As compared to D-001, NZP showed more preferable adsorption toward both toxic metals from the background Ca(II) solution at greater levels. The synthetic Pb(II) or Cd(II) solution containing other ubiquitous metal ions was employed as the feeding influent for column adsorption, and the results indicated that the treatable volume of NZP is around 3−4 times that of D-001 before reaching the breakthrough point set according to the effluent discharge standard of China. With respect to Pb(II) removal from an acidic mining effluent, the treatable volume of NZP was 13 times higher than that of D-001. The exhausted NZP could be effectively regenerated by HNO_3−$Ca(NO_3)_2$ binary solution for repeated use without any significant capacity loss. The superior performance of NZP was attributed to the Donnan membrane effect exerted by the host D-001 as well as the impregnated HZO nanoparticles of specific interaction toward toxic metals, as confirmed by the comparative isothermal adsorption and X-ray photoelectron spectroscopic study.

KEYWORDS: *hydrated zirconium oxide, polymeric nanocomposite, heavy metals, enhanced removal, XPS study, acidic mining effluent*

1. INTRODUCTION

Water and wastewater contaminated by heavy metals is a worldwide environmental concern because of their adverse impact on environmental ecosystems and public health. Various technologies such as chemical precipitation,[1] adsorption[2] and electrochemical method,[3] membrane filtration,[4] and biological treatment[5] have been proposed in response to heavy metal contamination. Among the available technologies, adsorption is regarded as one of the most attractive options and has been widely used in field application. Though various adsorbents have been fabricated for heavy metals such as ion exchangers, activated carbon, and numerous low-cost adsorbents, development of new adsorbent materials is still a hot topic because the available adsorbents have some inherent disadvantages from technical and economical viewpoints. For example, the polymeric ion exchangers usually trap heavy metals through nonspecific electrostatic interaction and thus display little or insufficient specific adsorption affinity toward the target metals in the presence of co-ions (e.g., Ca(II), Mg(II), etc.) at greater levels.[6] As a result, a significant decrease in the working capacity occurs, resulting in frequent regeneration and high operation cost.

In the past decades, various metallic oxides including Fe(III),[7] Mn(IV),[8] Ce(IV),[9] and Ti(IV)[10] oxides have been exploited as specific adsorbents through inner-sphere complexation with the target toxic metals. Similar to other metal oxides, hydrous Zr(IV) oxide ($ZrO_2 \cdot nH_2O$, HZO) could serve as a heavy metal adsorbent because it possess a rich amount of hydroxyl groups and shows high capacity and specific adsorption toward heavy metals such as Zn(II), Hg(II), Cd(II), and Sn(II).[11−14] Also, the exhausted HZO could be efficiently regenerated by acidic solution[12] because, as an amphoteric

Received: September 17, 2013
Accepted: October 29, 2013
Published: October 29, 2013

compound, HZO could be protonated or deprotonated at different pHs, with its pK_{pzc} value around 2.2−2.9.[14,15] Moreover, HZO is innocuous, inexpensive, and readily available, has good resistance to oxidant, and is very stable in a wide pH range (2−14),[16,17] implying its great potential in decontamination of water from toxic metals.

Unfortunately, as compared to Fe, Mn, and other metal oxides, less attention was paid to HZO to examine its properties and evaluate its potential in environmental application, possibly because HZO is scarcely present in natural environments such as in soils. Also, similar to other metal oxides, HZO is usually present as fine or ultrafine particles (micrometer level), and cannot be used directly in fixed bed or any other flow-through systems due to the excessive pressure drop and poor mechanical rigidity.

An effective approach to improve the applicability of fine metal oxide particles in water treatment is to impregnate them inside porous materials of larger size, such as activated carbon,[18] zeolite,[19] cellulose,[20] and some low-cost adsorbents.[21] The resultant composite adsorbents combine the specific adsorption of toxic metals by metal oxides with the advantage of the hosts with the improved permeability and feasible phase separation in flow-through systems. Recently, polymeric ion exchangers have been demonstrated as preferable host alternatives for metal oxide immobilization. It is originated from satisfactory mechanical rigidity of the polymeric hosts, as well as the potential Donnan membrane effect exerted by the immobilized charged groups covalently bound to the polymeric backbones, where target metal ions would be subjected to preconcentration and enhanced permeation prior to their effective sequestration by oxide particles.[22] Also, due to the crosslinking nature and nanoporous structure of the host polymer, the metal oxides could disperse as nanoparticles with larger specific surface areas and higher surface free energy, which would greatly favor heavy metal retention as compared to the bulky particles.[23]

The main objective of the current study is to develop a HZO-based nanocomposite adsorbent and evaluate its properties for efficient removal of toxic metals from water. A commercially available cation exchanger D-001 of porous polystyrene structure was employed as the host to immobilize HZO nanoparticles, and we obtained the resultant nanocomposite NZP. The physicochemical properties of NZP beads were characterized. Lead and cadmium ions were selected as the target pollutants because of their ubiquities in waters and negative impact on the environment. The influence of solution pH, adsorption time, and co-ions on adsorption was evaluated, and cyclic adsorption and regeneration experiments were performed to evaluate the newly developed adsorbent for lead and cadmium removal from water. The underlying adsorption mechanism was explored with the aid of X-ray photoelectron spectroscopy (XPS). Furthermore, wastewater from a local mineral processing plant was sampled for column tests to validate the feasibility of NZP for practical application.

2. MATERIALS AND METHODS

2.1. Materials. All chemicals of analytical grade or more pure were used in the current study without further purification. Stock solutions of Pb(II) and Cd(II) were prepared by dissolving $Pb(NO_3)_2$ and $Cd(NO_3)_2$ into ultrapure water, respectively. The macroporous polystyrene cation exchanger D-001 was kindly provided by Jiangsu NJU Environmental Technology Co., Ltd. Prior to use, the spherical D-001 beads were sieved (0.6−1.0 mm) and subjected to extraction with ethanol in a Soxhlet apparatus to remove the residue impurities, transferred to Na^+-type in NaOH solution, and then flushed with the ultrapure water until the neutral pH (6.8−7.2) was reached. Finally, the beads were vacuum dried at 343 K until a constant weight was reached. The bulky HZO particles were prepared by direct liquid precipitation and thermal treatment for comparative study.[12,24]

2.2. Fabrication of NZP. In brief, the preparation procedure of NZP consisted of the following three steps:

(i) Ten grams of D-001 beads was soaked into a 100 mL solution containing 25 g of ethanol and 10 g of $ZrOCl_2$. The mixture was stirred for 12 h to allow the uptake of Zr(IV) ions onto the inner surface of D-001 through a typical ion exchange process:

$$R{-}SO_3^-Na^+ + Zr^{4+} \rightarrow (R{-}SO_3^-)_4Zr^{4+} + Na^+ \quad (1)$$

(ii) The Zr(IV)-preloaded D-001 beads were filtered, desiccated under ambient temperature, transferred to a binary NaOH−NaCl solution (at 10% w/v concentration), and stirred for 12 h. Zr(IV) was then precipitated as Zr(IV) hydroxides onto the inner surface of D-001:

$$(R{-}SO_3^-)_4Zr^{4+} + NaOH + NaCl \rightarrow R{-}SO_3^-Na^+ + Cl^- + Zr(OH)_4\downarrow \quad (2)$$

(iii) The D-001 beads containing $Zr(OH)_4$ were dried at 60 °C for 12 h, and then the nanocomposite adsorbent NZP was obtained.

$$Zr(OH)_4 \xrightarrow{\Delta} ZrO_2{\cdot}nH_2O + H_2O\uparrow \quad (3)$$

2.3. Batch Adsorption Experiments. Batch adsorption experiments were conducted by using the traditional bottle-point method. Fifty milligrams of the adsorbent samples (D-001 or NZP) were equilibrated in 250 mL flasks with 100 mL of aqueous solutions containing Pb(II) or Cd(II) at designed levels. To study the effect of pH and coexisting Ca(II) on the metal uptake, the initial concentration of Pb(II) or Cd(II) was set as 0.5 mmol/L. In the isothermal study, the range of initial concentration of Pb(II) or Cd(II) was set from 0.25 to 4.0 mmol/L. The flasks were then transferred to a model G-25 incubator shaker with thermostat (New Brunswick Scientific Co., Inc.) and shaken at 150 rpm for 24 h at a given temperature. Ca(II) was employed as a competing ion by introducing a certain amount of $Ca(NO_3)_2$ into the test solution. HNO_3 and NaOH solutions were used to adjust the solution pH throughout the experiment when needed. Adsorption kinetics was performed by mixing a 1000 mL solution that contained 3.0 mmol Pb(II) or Cd(II) and 0.50 g of NZP and determined by sampling 0.5 mL aliquots at various time intervals. The effect of solution pH on the Zr leaching from NZP was examined as compared to the bulky HZO. The uptake of the target metals was determined by conducting a mass balance. Other details about batch adsorption were described in related tables and figures.

2.4. Fixed-Bed Column Sorption. Column adsorption experiments were carried out with a polyethylene column (12 mm diameter and 130 mm length) equipped with a water bath to maintain a constant temperature. The Lange-580 pumps (Baoding, China) were used to ensure a constant flow rate. The wet D001 or NZP beads of 5 mL were packed inside separate columns before operation. A synthetic feeding solution containing 20 mg/L Pb(II) or 5 mg/L Cd(II) and other co-ions (Ca(II), Mg(II), and Na(I)) was prepared. Its detailed composition is described in the related figures. The mining effluent was sampled from Nanjing Yinmao lead−zinc mining Co., Inc. and employed for column test to further validate the feasibility of NZP in wastewater treatment. The hydrodynamic conditions (i.e., a superficial liquid velocity (SLV) of 0.45 m/h and an empty bed contact time (EBCT) of 6.0 min) were identical for all the column adsorption runs. As for the regeneration test, the binary HNO_3(0.10 M)−$Ca(NO_3)_2$ (5 wt %) solution was used as the regenerant, and SLV and EBCT were set as 0.045 m/h and 60 min, respectively.

2.5. Characterization and Analysis. The specific surface area and pore size distribution of NZP was measured using N_2 adsorption and desorption tests at 77 K (Micromeritics ASAP-2010C). The morphology of the encapsulated Zr(IV) oxides was observed with transmission electron microscopy (JEM-200CX) equipped with a Gatan CCD camera working at accelerating voltage of 200 kV. The mineralogy of Zr(IV) oxides was determined by powder X-ray diffraction patterns over a wide range of angles (10−80°) using a high-resolution X-ray diffractometer (XTRA) with Cu Kα radiation (40 kV, 25 mA). An inductive coupled plasma (ICP) emission spectrometer (PerkinElmer Model Optima 5300DV) was used to determine the Zr concentration in solution, and the Zr amount loaded within D-001 was measured after the nancomposite sample was digested into a HNO_3−$HClO_4$ solution. The Pb(II) and Cd(II) concentration in solution was determined by a Shimadzu AA-6800 atomic absorption/emission spectrometer equipped with a graphite furnace atomizer and deuterium background correction. The Pb(II) adsorbed samples were vacuum desiccated at 323 K for 24 h and then ground into powder for further X-ray photoelectron spectroscopy (XPS) analysis (UlVAC-PHI model 5000 Versa probe). All the binding energies were referenced to the C 1s peak at 284.8 eV to compensate for the surface charging effects. The XPS results were collected as binding energy forms and fitted using a curve-fitting program (XPSpeak4.1).

3. RESULTS AND DISCUSSION

3.1. Characterization of NZP. The resulting nanocomposite adsorbent NZP was present as spherical beads of brownish-yellow color. As shown in Figure 1a, the TEM image suggests that HZO was immobilized inside D-001 as nanoparticles (10−20 nm). Nanosized metal oxides usually display larger accessible surface areas and higher surface free energy than the bulky ones, and thus are expected to offer more active adsorption sites.[25] According to the wide-angle XRD patterns of NZP, D-001, and the bulky HZO particles (Figure 1b), most HZO impregnated inside D-001 is amorphous in nature. It possibly resulted from the relatively low temperature (<100 °C) during the preparation process.[24] The basic structure of NZP could be schematically illustrated as Figure 3c.

The basic properties of NZP and D-001 were summarized in Table 1. The amount of Zr loaded within D-001 was determined as 16.0% in Zr mass, resulting in a higher apparent density of NZP than D-001. Due to the pore clogging caused by HZO encapsulation, both the average pore diameter and pore volume of NZP fell down. However, a slight increase in the surface area from 18.2 to 20.4 m^2/g is possibly caused by the presence of the HZO nanoparticles of higher surface areas. From the N_2 adsorption−desorption isotherm on NZP at 77 K, the hysteresis loop was observed in the range 0.9−1.0 of P/P_0 (Figure S1, Supporting Information), indicating the meso- to macroporous nature of NZP.

The effect of solution pH on the stability of NZP and the bulky HZO is compared and described in Figure 2. Both NZP and HZO are stable at a solution pH higher than 3. A slight Zr leaching (1.4%) from HZO was observed when the pH decreased from 3 to 1, and no Zr leaching occurred for NZP under the identical conditions. Further decrease of the pH from 1 to 0.3 resulted in a significant Zr leaching from both adsorbents, and much higher Zr leaching at a pH of 0.30 was detected for HZO (11.7%) than for NZP (5.0%). All the above results indicated that the host D-001 could help to inhibit HZO leaching into solution, though nanosized metal oxide particles tend to dissolve into water more readily than the bulky one.[26] A similar favorable result was observed in our previous study when immobilizing hydrated ferric oxide was immobilized inside a polymeric exchanger.[27] Compared with other metal oxide-contained nanocomposite adsorbents, NZP exhibited much better acidic resistance. For instance, almost all the Fe(III) oxide encapsulated inside D-001 was dissolved and leached into solution at pH = 1.0 for 24 h.[28] Such performance of NZO is very attractive because heavy metals are usually present in acidic wastewater such as, for instance, acidic mining effluents discharged from mining plants.

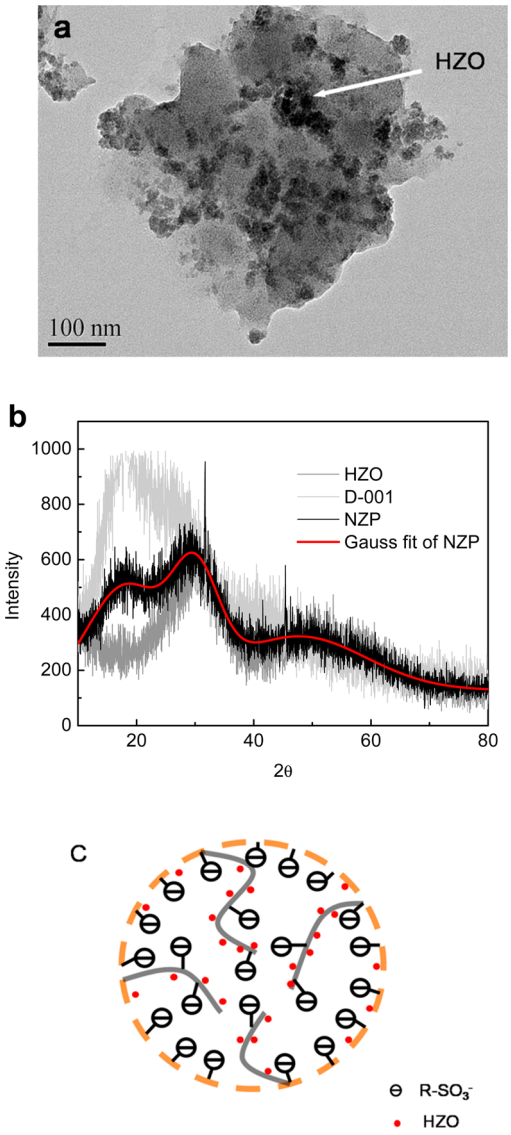

Figure 1. Characterization of NZP: (a) TEM image of NZP; (b) XRD spectra of HZO particles, D-001, and NZP. (c) Schematic illustration of NZP.

Table 1. Physicochemical Properties of Two Polystyrene-Based Adsorbents

adsorbent	D-001	NZP
matrix	polystyrene	
functional sites	$-SO_3^-Na^+$	$-SO_3^-Na^+$; HZO
BET surface area (m^2/g)	18.2	20.4
pore volume (cm^3/g)	0.185	0.156
average pore diameter (nm)	31.9	27.2
apparent density (g/cm^3)	0.56	0.74

3.2. Effect of Solution pH. The effect of solution pH on Pb(II) and Cd(II) uptake was examined, and the results are

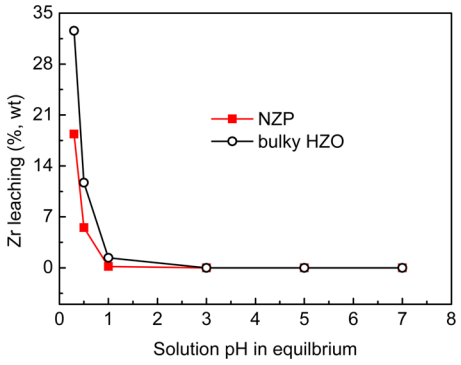

Figure 2. pH-dependent Zr leaching from NZP and bulky HZO particles (96 h shaking at 303 K).

presented in Figure 3. Both Pb(II) and Cd(II) uptake increased when the solution pH was increased from 1.0 to 6.0, and higher

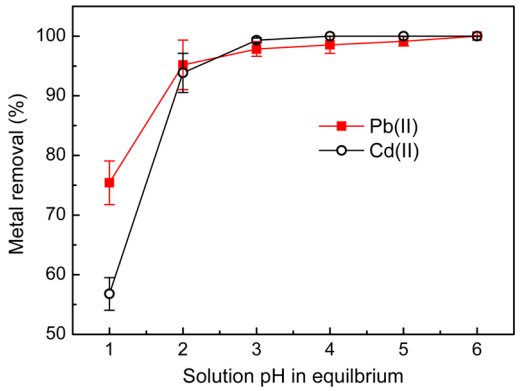

Figure 3. Effect of solution pH on Pb(II) and Cd(II) removal by NZP at 303 K. Initial M(II) = 0.5 mM, S/L = 0.5 g/L.

values were not tested to avoid the metal precipitation. The pH-dependent removal of both metals could be explained on the basis of the NZP structure. NZP is composed of the host resin D-001 and the impregnated HZO nanoparticles, and the sulfonate groups binding to the D-001 matrix could sequester lead and cadmium ions through nonspecific electrostatic interaction, while the entrapped HZO nanoparticles could exhibit specific interactions with the target metals.[29] Metal adsorption onto D-001 (Na-type) can be represented by the following reactions:

$$2R{-}SO_3Na + M^{2+} \rightarrow (R{-}SO_3)_2M + 2Na^+ \quad (4)$$

$$(R{-}SO_3)_2M + 2H^+ \rightarrow 2R{-}SO_3H + M^{2+} \quad (5)$$

whereas M(II) retention by HZO could be described as the following two reactions:[12]

$$(\equiv Zr{-}OH)_2 + M^{2+} \rightarrow 2(\equiv Zr{-}O){-}M + 2H^+ \quad (6)$$

$$=Zr{-}(OH)_2 + M^{2+} \rightarrow =Zr{-}(O)_2{-}M + 2H^+ \quad (7)$$

Obviously, a low pH value or high acidity would abate Pb(II) or Cd(II) retention through H^+ competition, as suggested by eqs 5−7. Of note is that NZP still exhibited satisfactory retention of Pb(II) and Cd(II) at a low pH (e.g., 2), whereas for other adsorbents, like ion exchangers or those modified by N, O, or S-contained groups, their adsorption towards toxic metals are always inhibited in acidic pHs because of the H^+ competition or protonation of the functional groups.[30] Such attractive performance of NZP possibly resulted from the relatively low pH_{pzc} value of HZO around 2.2−2.9,[14,15] and at pH higher than the pH_{pzc}, the metal ions are expected to be effectively adsorbed onto HZO surface. On the basis of the results described in Figures 2 and 3, the pH-dependent stability and adsorption of NZP implies the possibility to regenerate the exhausted nanocomposite by using acidic solution at pH around 1, which is demonstrated in the following section.

3.3. Adsorption Kinetics. Adsorption kinetics of Pb(II) and Cd(II) on NZP and D-001 were examined, and the results are presented in Figure 4. An initial fast adsorption was

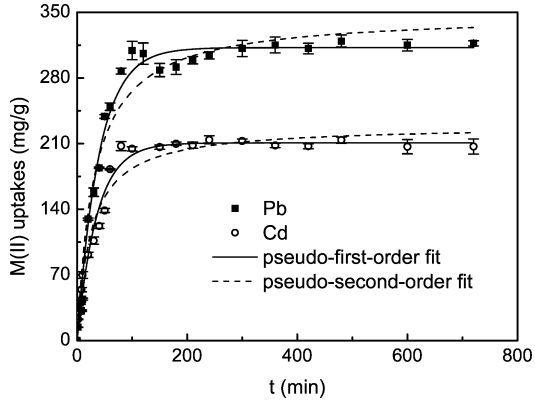

Figure 4. Adsorption kinetics of heavy metal ions onto NZP at 303 K. Initial M(II) = 3.0 mM, pH = 5.3 ± 0.1.

observed for both metals, followed by a slow stage, and the adsorption equilibrium was achieved within 200 min for Pb(II) and 100 min for Cd(II), respectively. Kinetic data for both metals were represented by pseudo-first- or pseudo-second-order as

$$\log(q_e - q_t) = \log q_e - \frac{k_1}{2.303}t \quad (8)$$

$$\frac{t}{q_t} = \frac{1}{k_2 q_e^{\,2}} + \frac{t}{q_e} \quad (9)$$

where t (min) is the adsorption period, q_t (mg/g) and q_e (mg/g) are the adsorption capacities at time t and equilibrium respectively, and k_1 (min^{-1}) and k_2 ($L{\cdot}min^{-1}{\cdot}g^{-1}$) are the rate constants of the pseudo-first or pseudo-second-kinetic model, respectively.

High correlation coefficients and the calculated q_e values (Table 2) close to the experimental data indicated that both lead and cadmium uptake onto NZP can be approximated by the pseudo-first-order model more reasonably. Also, the adsorption capacities of NZP for both metals were roughly compared with other adsorbents reported in the open literature (Table 3).

3.4. Effect of Calcium Ions. It is of particular significance to elucidate the preference of a given adsorbent toward toxic metals because Ca(II), Mg(II), or Na(I) ions are commonly present in natural waters or industrial effluents. Here, we tested the effect of Ca(II) on the uptake of Pb(II) and Cd(II) onto NZP. Ca(II) was selected as a representative background ion because it shows a stronger competitive effect on heavy metal retention than Mg(II) or Na(I) ions.[37,38] The host ion exchanger D-001 was involved for comparison purpose. As

Table 2. Kinetic Parameters for Pb(II) and Cd(II) Uptake onto NZP at 303 K

	pseudo-first-order			pseudo-second-order			
heavy metals	k_1 (min)	q_e (mg/g)	R^2	k_2 (10^{-4}L·min^{-1}·mg^{-1})	q_e (mg/g)	R^2	experimental q_m (mg/g)
Pb(II)	0.058	312	0.988	0.929	348	0.969	319.4 ± 6.4
Cd(II)	0.064	211	0.981	1.745	229	0.969	213.7 ± 3.5

Table 3. Comparison of Adsorption Capacities of Various Adsorbents toward Pb(II) and Cd(II)

	adsorption capacity (mg/g)		
adsorbents	Pb	Cd	reference
chelating resin functionalized with dithiooxamide	24.3	9.0	31
poly(MMA–MAGA) functionalized with methacryloylamidoglutamic acid groups	65.2	28.2	32
poly(styrene-*co*-divinylbenzene)amine	73.0		33
cellulose–manganese oxide hybrid material	80.1		20
polyhedral oligomeric silsesquioxanes (POSS) incorporated with Fe_3O_4	90.9		34
EGTA-modified chitosan	101.4	83.2	35
polyacrylamide-hydrated ferric oxide hybrid material	211.4	147.2	36
NZP	319.4	214.7	this study

illustrated in Figure 5, when the molar amount of Ca(II) was increased from 0 to 80 times that of Pb(II) or Cd(II), the

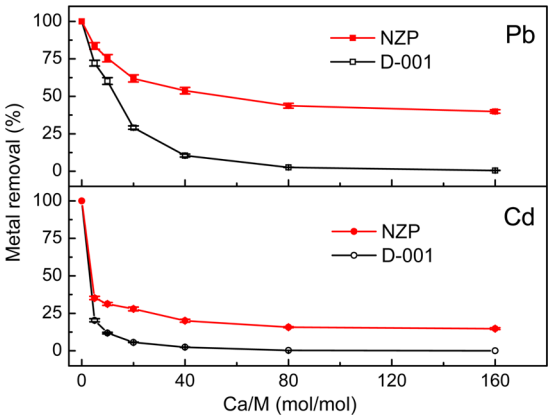

Figure 5. Effect of Ca(II) on uptake of Pb(II) and Cd(II) onto NZP at 303 K. Initial M(II) = 0.5 mM, S/L = 0.5 g/L, pH = 5.3 ± 0.1.

retention of both Pb(II) and Cd(II) by D-001 decreased dramatically to nearly zero, whereas the NZP still performed 43.75% removal for Pb(II) and 15.77% for Cd(II). Generally speaking, NZP exhibited higher efficiency for Pb(II) or Cd(II) retention than D-001 in the presence of Ca(II). This is because the sulfonate groups of D-001 sequester Pb(II) or Cd(II) ions through nonspecific electrostatic interactions, and the added Ca(II) greatly competes for sulfonate groups of D-001, whereas the encapsulated HZO nanoparticles are believed to sequester heavy metal ions by specific inner-sphere complexation.[12,29]

To quantify the adsorption preference of NZP, the distribution coefficient, K_d, of NZP and D-001 toward Pb(II) and Cd(II) in the presence of different Ca(II) levels were calculated according to eq 10 and listed in Table 4:

$$K_d = \frac{(C_0 - C_e)}{C_e} \times \frac{V}{m} \quad (10)$$

Table 4. K_d (L/g) Values of Pb(II) and Cd(II) Adsorbed by NZP and D-001 in the Presence of Ca(II) at Different Levels

		K_d (L/g) at different initial Ca/M molar ratios					
heavy metals (M)	adsorbent	5	10	20	40	80	160
Pb(II)	NZP	10.16	6.14	3.25	2.33	1.56	1.33
	D-001	5.17	3.02	0.82	0.23	0.05	0.01
Cd(II)	NZP	1.09	0.91	0.78	0.50	0.37	0.35
	D-001	0.51	0.27	0.12	0.05	0.01	0.00

where K_d (L/g) is the distribution coefficient, C_0 (mg/L) and C_e (mg/L) are the initial and equilibrium concentrations of metal ions respectively, V (L) is the volume of solution, and m (g) is the mass of sorbent.

The substantially larger K_d values of Pb(II) than Cd(II) indicate more preferable adsorption of Pb(II) than Cd(II). As inferred from the structure of NZP (Figure 1c), Pb(II) and Cd(II) adsorption by NZP can be realized through two different pathways (i.e., ion exchange with the sulfonate groups of the host D-001 and the inner-sphere complexation with the loaded HZO nanoparticles). The ion exchange preference is greatly dependent upon the Gibbs free energies of the hydration of target ions, and divalent cations with lower hydration energies (i.e., Pb(II) (−1425 kJ/mol)) are adsorbed preferably over those with higher hydration energies (i.e., Cd(II) (−1755 kJ/mol)).[37−39] The inner-sphere complexation can be roughly explained by the principle of hard and soft acids and bases (the HSAB principle). HZO nanoparticles are supposed to act as a soft Lewis base and the heavy metal ions act as soft Lewis acid. The larger ionic radius of Pb(II) results in its higher softness than Cd(II).[22,38] Thus, Pb(II) is more preferably adsorbed onto NZP than Cd(II).

3.5. Adsorption Mechanism. Preferable adsorption of Pb(II) and Cd(II) ions over Ca(II) ions by NZP can be elucidated on the basis of its specific two-site structure, as illustrated in Figure 1c. As discussed above, the immobilized sulfonate groups covalently bound to the polystyrene matrix of D-001 could enhance preconcentration and permeation of target ions prior to their effective sequestration by the inside oxide particles, which is the so-called Donnan effect.[40] Also, the entrapped HZO nanoparticles would propose a specific metal coordination with target ions (i.e., the inner-sphere surface complexation).[29]

The favorable role of the sulfonate groups in heavy metal sequestration by the loaded HZO nanoparticles was preliminarily demonstrated by comparing the performance of the nanocomposite adsorbent and its corresponding mixture of bulky HZO particles and D-001, and the results are shown in Figure 6a,b. The background Ca(II) at 1600 mg/L in solution was designed to fully screen the possible heavy metal retention by the sulfonate groups of D-001, as proved by the pre-experiment. In the test concentration ranges, the nanocomposite NZP exhibits more efficient removal of both toxic metals than a simple binary mixture of HZO and D-001,

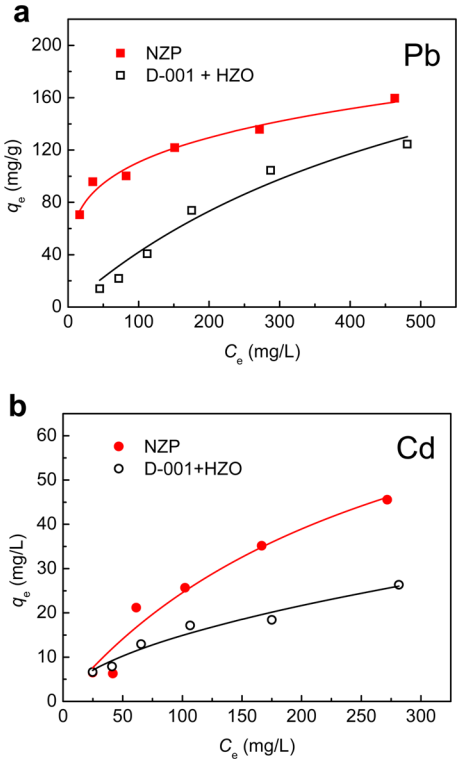

Figure 6. Heavy metal adsorption onto NZP and the binary adsorbent (D-001 + HZO particles) at 303 K: (a) Pb(II); (b) Cd(II). Solid dosage: NZP 0.50 g/L or 0.36 g/L D-001 + 0.14 g/L HZO. Note that Zr content for both adsorbents was equal.

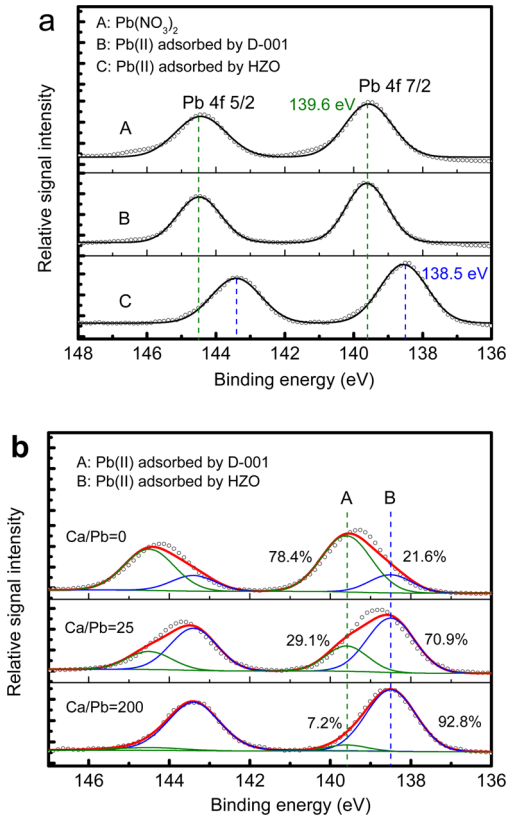

Figure 7. High-resolution XPS spectra of Pb 4f: (a) Pb(II)-adsorbed D-001 and Pb(II)-adsorbed HZO; (b) Pb(II)-loaded NZP sampled from solution of differentCa(II)/Pb(II) molar ratios. Initial Pb(II) = 0.5 mmol/L, adsorbent dosage was 0.50 g/L, pH = 5.3 ± 0.1, T = 303 K.

indicating that the host D-001 plays a favorable role in metal sequestration by the entrapped HZO nanoparticles.

Furthermore, an XPS study was performed on the Pb(II)-preloaded adsorbent to distinguish the different role of two adsorption sites of NZP (i.e., the sulfonate groups of the host and HZO nanoparticles). As seen in Figure 7a, the peaks of binding energy for Pb(II) adsorbed by D-001 are centered at 144.5 eV for Pb 4f5/2 and 139.6 eV for Pb 4f7/2, respectively, the same as the Pb(II) binding energy of $Pb(NO_3)_2$. Contrarily, a remarkable shift to lower binding energy of Pb 4f was observed when Pb(II) was adsorbed onto HZO particles, indicating that Pb(II)−HZO interaction is specific and much stronger than the electrostatic attraction between Pb(II) and D-001.

Also, an XPS study was performed on three NZPs sampled from a solution of different Ca(II)/Pb(II) molar levels to reveal how Ca(II) affected Pb(II) retention by NZP, and the results are illustrated in Figure 7b. With an increase in the Ca(II)/Pb(II) molar ratio from 0 to 200, the relative area of peak A, which corresponds to Pb 4f7/2 adsorbed by D-001, decreased significantly from 78.4% to 7.2%, while that of peak B, which corresponds to Pb 4f7/2 adsorbed by loaded HZO nanoparticles, increased from 21.6% to 92.8%. A similar tendency was also observed for Pb 4f5/2. Such interesting observations further demonstrated that Pb(II) adsorbed by the sulfonate groups was greatly inhibited by the addition of Ca(II), and Pb(II) retention by HZO dominated the total metal adsorption of NZP at high Ca(II) levels.

3.6. Fixed-Bed Adsorption. A fixed-bed column adsorption experiment was conducted to evaluate the applicability of a given adsorbent in water treatment. Figure 8a,b illustrated an effluent history of separate fixed-bed columns packed with either NZP or D-001 for simulated feeding solutions that contained Pb(II) or Cd(II) ions with other ubiquitous ions including Na(I), Ca(II), and Mg(II). The breakthrough point was set as 1 mg/L for Pb(II) and 0.1 mg/L for Cd(II), as recommended by the integrated wastewater discharge standard of China.[41] The treatable volume of NZP is about 1750 and 270 bed volume (BV) for Pb(II) and Cd(II), respectively, whereas only 600 and 80 BV of D-001. Furthermore, Pb(II) and Cd(II) retention by NZP could result in both toxic metals to meet the drinking water standards recommended by the World Health Organization (10 μg/L for Pb and 5 μg/L for Cd).[42]

In situ regeneration of the exhausted NZP column was performed by using the binary HNO_3 (0.1 M) + $Ca(NO_3)_2$ (5 wt %) solution at 298 K. As seen in Figure 9a,b, the preloaded Pb(II) and Cd(II) by NZP could be effectively desorbed with the regeneration efficiency >95%. Before the next cycle adsorption, both NZP columns were rinsed with 3 BV 0.10 M NaOH solution to neutralize the protonated HZO and transfer D-001 from H-type to Na-type. Cyclic adsorption and regeneration runs of the NZP columns were performed to validate their repeatability for heavy metal removal. The overlap of the cyclic breakthrough curves illustrated in Figure 8a,b demonstrated that NZP could be employed for repeatable Pb(II) and Cd(II) removal without any significant capacity loss.

We also sampled acidic mining effluent from a mining plant in Nanjing and examined the feasibility of NZP for industrial wastewater treatment. Detailed composition of the feeding wastewater was described in Figure 10a. The breakthrough

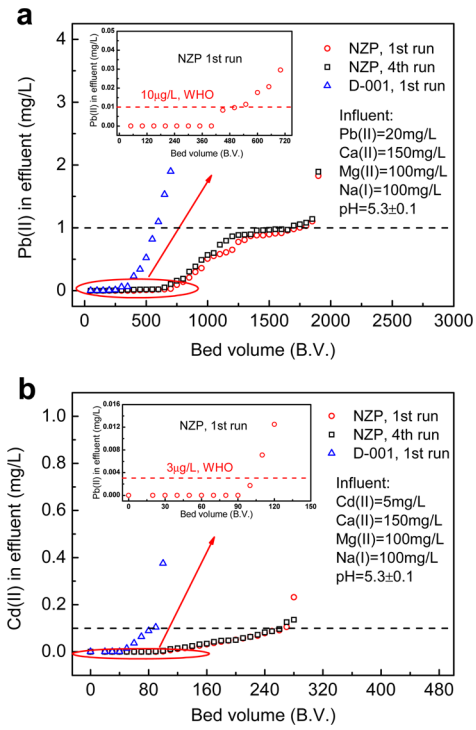

Figure 8. Breakthrough curves of (a) Pb(II) and (b) Cd(II) adsorption from synthetic wastewaters onto NZP and D-001 at 298 K. Superficial liquid velocity (SLV) = 0.45 m/h. Empty bed contact time (EBCT) = 6.0 min.

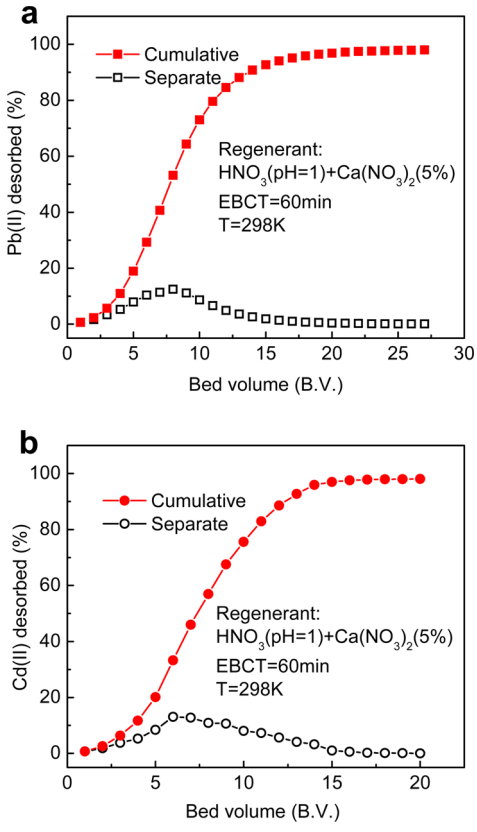

Figure 9. In situ regeneration of the exhausted columns packed with NZP: (a) Pb(II); (b) Cd(II).

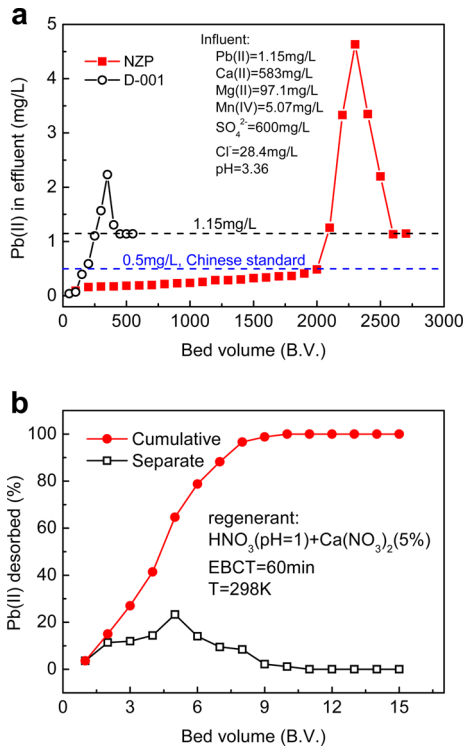

Figure 10. Fixed-bed column retention of Pb(II) from practical mining drainage: (a) adsorption by NZP or D-001; (b) regeneration of the exhausted NZP column.

point was set as 0.5 mg/L Pb(II), the maximum concentration level regulated by the mining industry emission standard of China.[43] Results indicated that the effective treatable volume of NZP was around 2000 BV, whereas that of D-001 was only 150 BV. Also, other toxic metals including Cr(III) and Cu(II) initially at 0.026 and 0.690 mg/L, respectively, were completely eliminated by NZP adsorption. Note that for the breakthrough curves of both D-001 and NZP columns, higher Pb(II) concentration in effluent than in the feeding solution occurred after reaching the breakthrough point. Similar results were reported earlier[44] and could be ascribed to the chromatographic elution effect of Pb(II) by other coexisting ions. In other words, a fraction of Pb(II) initially loaded on both adsorbents was jostled by other co-ions when insufficient adsorption sites were available. The binary HNO_3 (0.1 M) + $Ca(NO_3)_2$ (5 wt %) solution was used to regenerate the exhausted NZP with the efficiency higher than 95%. The results further suggested the potential of NZP for enhanced removal of heavy metals from industrial wastewaters.

4. CONCLUSION

Nanosized hydrous zirconium oxide could be encapsulated inside a polymeric cation exchanger D-001 to improve its applicability for decontamination of water from heavy metals like lead and cadmium. The resultant nanocomposite adsorbent NZP could effectively capture both toxic metals in pH 2−6 without any Zr(IV) leaching from the NZP, and it was achieved through two distinct processes: nonspecific ion exchange by the sulfonate groups of D-001 and specific inner-sphere complexation by the entrapped HZO nanoparticles. Consequently, NZP exhibited preferable adsorption to both toxic metals than other co-ions like calcium. Cyclic column adsorption tests that used the synthetic and real acidic mining effluent as the feeding

solution further demonstrated that NZP could be employed for repeated use without any capacity loss, when the binary HNO_3–$Ca(NO_3)_2$ solution was employed as the regenerant.

■ ASSOCIATED CONTENT

Supporting Information

N_2 adsorption–desorption isotherms by NZP at 77 K; isotherm constants for Pb(II) and Cd(II) uptake onto NZP at 303 K; adsorption isotherms of (a) Pb(II) and (b) Cd(II) by NZP at 303 K. This material is available free of charge via the Internet at http://pubs.acs.org.

■ AUTHOR INFORMATION

Corresponding Author

*B. Pan. E-mail: bcpan@nju.edu.cn. Tel: +86-25-8968-0390.

Notes

The authors declare no competing financial interest.

■ ACKNOWLEDGMENTS

The study was financially supported by Jiangsu NSF (BK2012017), NSFC (21177059), and Changjiang Scholars Innovative Research Team in University (IRT1019)

■ REFERENCES

(1) Fu, F. L.; Xie, L. P.; Tang, B.; Wang, Q.; Jiang, S. X. *Chem. Eng. J. (Amsterdam, Neth.)* **2012**, *189*, 283–287.
(2) El-Shahat, M. F.; Shehata, A. M. A. *Asian J. Chem.* **2013**, *25*, 4284–4288.
(3) Bayar, S.; Yilmaz, A. E.; Boncukcuoglu, R.; Fil, B. A.; Kocakerim, M. M. *Desalin. Water Treat.* **2013**, *51*, 2635–2643.
(4) Llanos, J.; Williams, P. M.; Cheng, S.; Rogers, D.; Wright, C.; Perez, A.; Canizares, P. *Water Res.* **2010**, *44*, 3522–3530.
(5) Reddad, Z.; Gerente, C.; Andres, Y.; Le Cloirec, P. *Environ. Sci. Technol.* **2012**, *36*, 2067–2073.
(6) Fu, F. L.; Wang, Q. *J. Environ. Manage.* **2011**, *92*, 407–418.
(7) Hu, J.; Chen, G. H.; Lo, I. M. C. *J. Environ. Eng.* **2006**, *132*, 709–715.
(8) Su, Q.; Pan, B. C.; Wan, S. L.; Zhang, W. M.; Lv, L. *J. Colloid Interface Sci.* **2010**, *349*, 607–612.
(9) Recillas, S.; Colon, J.; Casals, E.; Gonzalez, E.; Puntes, V.; Sanchez, A.; Font, X. *J. Hazard. Mater.* **2010**, *184*, 425–431.
(10) Debnath, S.; Nandi, D.; Ghosh, U. C. *J. Chem. Eng. Data* **2011**, *56*, 3021–3028.
(11) Mishra, S. P.; Singh, V. K.; Tiwari, D. *Appl. Radiat. Isot.* **1996**, *47*, 15–21.
(12) Mishra, S. P.; Singh, V. K.; Tiwari, D. *J. Radioanal. Nucl. Chem.* **1996**, *210*, 207–217.
(13) Mishra, S. P.; Singh, V. K.; Tiwari, D. *Radiochim. Acta* **1997**, *76*, 97–101.
(14) Venkatesan, K. A.; Selvam, G. P.; Rao, P. R. V. *Sep. Sci. Technol. (Philadelphia, PA, U. S.)* **2000**, *35*, 2343–2357.
(15) Rodrigues, L. A.; Maschio, L. J.; da Silva, R. E.; da Silva, M. *J. Hazard. Mater.* **2010**, *173*, 630–636.
(16) Bergamaschi, V. S.; Carvalho, F. M. S.; Rodrigues, C.; Fernandes, D. B. *Chem. Eng. J.* **2005**, *112*, 153–158.
(17) Rodrigues, L. A.; Maschio, L. J.; Coppio, L. D. C.; Thim, G. P.; da Silva, M. *Environ. Technol.* **2012**, *33*, 1345–1351.
(18) Mackenzie, K.; Bleyl, S.; Georgi, A.; Kopinke, F. D. *Water Res.* **2012**, *46*, 3817–3826.
(19) Liu, H. B.; Peng, S. C.; Shu, L.; Chen, T. H.; Bao, T.; Frost, R. L. *Chemosphere* **2013**, *91*, 1539–1546.
(20) Maliyekkal, S. M.; Lisha, K. P.; Pradeep, T. *J. Hazard. Mater.* **2010**, *181*, 986–995.
(21) Kim, K. H.; Keller, A. A.; Yang, J. K. *Colloids Surf., A* **2013**, *425*, 6–14.
(22) Puttamraju, P.; SenGupta, A. K. *Ind. Eng. Chem. Res.* **2006**, *45*, 7737–7742.
(23) Savage, N.; Diallo, M. S. *J. Nanopart. Res.* **2005**, *7*, 331–342.
(24) Yoldas, B. E. *J. Mater. Sci.* **1986**, *21*, 1080–1086.
(25) Aditya, D.; Rohan, P.; Suresh, G. *Res. J. Chem. Environ.* **2011**, *15*, 1033–1040.
(26) Mudunkotuwa, I. A.; Rupasinghe, T.; Wu, C. M.; Grassian, V. H. *Langmuir* **2012**, *28*, 396–403.
(27) Nie, G. Z.; Pan, B. C.; Zhang, S. J.; Pan, B. J. *J. Phys. Chem. C* **2013**, *117*, 6201–6209.
(28) Pan, B. J; Qiu, H.; Pan, B. C.; Nie, G. Z.; Xiao, L. L.; Lv, L.; Zhang, W. M.; Zhang, Q. X.; Zheng, S. R. *Water Res.* **2010**, *44*, 815–824.
(29) Schmidt, G. T.; Vlasova, N.; Zuzaan, D.; Kersten, M.; Daus, B. *J. Colloid Interface Sci.* **2008**, *317*, 228–234.
(30) Febrianto, J.; Kosasih, A. N.; Sunarso, J.; Ju, Y. H.; Indraswati, N.; Ismadji, S. *J. Hazard. Mater.* **2009**, *162*, 616–645.
(31) Dutta, S.; Das, A. K. *J. Appl. Polym. Sci.* **2007**, *103*, 2281–2285.
(32) Denizli, A.; Sanli, N.; Garipcan, B.; Patir, S.; Alsancak, G. *Ind. Eng. Chem. Res.* **2004**, *43*, 6095–6101.
(33) Rivas, B. L.; Pooley, S. A.; Maturana, H. A.; Villegas, S. *J. Appl. Polym. Sci.* **2001**, *80*, 2123–2127.
(34) He, H. B.; Li, B.; Dong, J. P.; Lei, Y. Y.; Wang, T. L.; Yu, Q. W.; Feng, Y. Q.; Sun, Y. B. *ACS Appl. Mater. Interfaces* **2013**, *5*, 8058–8066.
(35) Zhao, F. P.; Repo, E.; Yin, D. L.; Sillanpaa, M. E. T. *J. Colloid Interface Sci.* **2013**, *409*, 174–182.
(36) Manju, G. N.; Krishnan, K. A.; Vinod, V. P.; Anirudhan, T. S. *J. Hazard. Mater.* **2002**, *91*, 221–238.
(37) Marcus, Y. *J. Chem. Soc., Faraday Trans.* **1991**, *87*, 2995–2999.
(38) Yuan, G.; Seyama, H.; Soma, M.; Theng, B. K. G.; Tanaka, A. *J. Environ. Sci. Health, Part A: Toxic/Hazard. Subst. Environ. Eng.* **1999**, *34*, 625–648.
(39) deNamor, A. F. D.; Chahine, S.; Kowalska, D.; Castellano, E. E.; Piro, O. E. *J. Am. Chem. Soc.* **2002**, *124*, 12824–12836.
(40) Sarkar, S.; Chatterjee, P. K.; Cumbal, L. H.; SenGupta, A. K. *Chem. Eng. J.* **2011**, *166*, 923–931.
(41) *Integrated Wastewater Discharge Standard*; Ministry of the People's Republic of China: Beijing, 1996.
(42) *Guidelines for Drinking-water Quality*, third ed.; World Health Organization: Geneva, 2008.
(43) *Emission Standard of Pollutants for Lead and Zinc Industry*; Ministry of the People's Republic of China: Beijing, 2010.
(44) Blaney, L. M.; Cinar, S.; SenGupta, A. K. *Water Res.* **2007**, *41*, 1603–1613.